Noguera-Díaz, A., Bimbo, N., Holyfield, L. T., Ahmet, I. Y., Ting, V. P., & Mays, T. J. (2016). Structure-property relationships in metal-organic frameworks for hydrogen storage. *Colloids and Surfaces A. Physicochemical and Engineering Aspects*, *496*, 77-85. https://doi.org/10.1016/j.colsurfa.2015.11.061

Supplementary information

Structure-property relationships in metal-organic frameworks for hydrogen storage

*Antonio Noguera-Díaz[1], Nuno Bimbo[1], Leighton T Holyfield[1,2], Ibbi Yilmaz Ahmet[2], Valeska P Ting[1] and Timothy J Mays[1]**

[1]Department of Chemical Engineering, University of Bath, Claverton Down, Bath, BA2 7AY, United Kingdom

[2]Doctoral Training Centre for Sustainable Chemical Technologies, University of Bath, Claverton Down, Bath, BA2 7AY, United Kingdom

Synthesis information

Materials were synthesized using different recipes from literature, being these scaled up in some cases [1-8]. HKUST-1 (Basolite^{TM} C300) was supplied by Sigma Aldrich.

IRMOF-1

3 Batches of IRMOF-1 [$Zn_4O(BDC)_3(DEF)_7(H_2O)_3$] were synthesized by using a modified synthesis from the patent from Yaghi *et al.* [3, 9]. Zinc nitrate hexahydrate (0.3570 g, 1.20 mmol) and terephthalic acid (known as 1,4-benzenedicarboxylic acid or H_2BDC) (0.066 g, 0.20 mmol) was dissolved in 10 mL of DEF (N,N-Diethylformamide) at 200 RPMs. The mix was placed in a hydrothermal bomb and heated in in the oven at a constant rate of 2 °C min^{-1} to 105 °C for 20 h. and then allowed to cool to room temperature.

IRMOF-3

5 Batches of IRMOF-3 [$Zn_4O(NH_2\text{-}BDC)_3(DEF)_7$] were made using the synthesis from Yaghi's *et al.* patent [3, 9]. Zinc nitrate hexahydrate (0.1790 g, 0.600 mmol) and 2-aminotherephthalic acid (0.0360 g) were dissolved in 9 mL of DEF and 3 mL of ethanol at 200 RPMs. The mix was placed in a hydrothermal bomb and put in the oven at a constant rate 2° C min^{-1} to 105° C for 20 h and it was allowed to cool to room temperature (RT):

IRMOF-9

2 Batches of IRMOF-9 [$Zn_4O(BPDC)_3(DEF)_7(H_2O)_4$] was obtained using a modified using the synthesis from Yaghi's patent [3, 9]. Zinc nitrate hexahydrate (0.110 g, 0.42 mmol) and 4,4'-biphenyldicarboxilic acid (0.08 g, 0.03 mmol) was dissolved in 10 mL of DEF at 200 RPMs. The mix was placed in a hydrothermal bomb and put in the oven at a constant rate 2° C min^{-1} at 100 °C for 48 h and it was allowed to cool to room temperature.

ZIF-7

A batch of ZIF-7 (SOD topology) ($Zn(C_7H_2N_2)_2 \cdot (H_2O)_3$) was successfully synthesized using a three times scaled-up protocol [10]. In the original synthesis, 0.1200 g (1 mmol) of bIm (benzimidazole) were dissolved in 6.8 g of ethanol. After, the ammonia hydroxide (28–30% aqueous solution, 0.18 g) and the zinc acetate dihydrate (0.1100 g, 0.5 mmol) were added to the mix. The solution was stirred at RT for 3 hours.

ZIF-8

ZIF-8 (SOD topology) [$(ZnC_8H_{10}N_4) \cdot 3.33(H_2O)$] was successfully synthesized using a protocol obtained from literature [5]. 1.460 g of zinc nitrate hexahydrate (4.91 mmol) were dissolved in 100 mL of methanol at the same time that 3.15 g of 2-methylimidazole (38.36 mmol) were dissolved in another beaker with 100 mL of methanol. The solution was stirred at RT for 3 hours.

ZIF-9

ZIF-9 (SOD topology) [$Co(C_7H_5N_2)_2 \cdot (H_2O)$] was successfully synthesized using a four times scaled-up protocol to ensure enough sample was obtained [10]. In the original synthesis, 0.1200 g (1 mmol) of bIm (benzimidazole) were dissolved in 6.9 g of ethanol. After, the ammonia hydroxide (28–30% aqueous solution, 0.18 g) and the cobalt acetate tetrahydrate (0.1250 g, 0.5 mmol) were added to the mix. The solution was stirred at RT for 3 hours.

ZIF-11

ZIF-11 (RHO topology) ($Zn(C_7H_5N_2)_2 \bullet 0.36(C_7H_8)$ was successfully synthesized using a three times scaled-up protocol to ensure enough sample was obtained [10]. In the original synthesis, 0.1200 g (1 mmol) of bIm (benzimidazole) were dissolved in 6.8 g of ethanol. After that, toluene (4.6 g, 50 mmol), ammonia hydroxide (28–30% aqueous solution, 0.18 g) and the zinc acetate dihydrate (0.1100 g, 0.5 mmol) were added to the mix. The solution was stirred at RT for 3 hours.

ZIF-12

ZIF-12 (RHO topology) ($Co(C_7H_5N_2)_2$) was successfully synthesized using a three times scaled-up protocol to ensure enough sample was obtained [10]. In the original synthesis, 0.1200 g (1 mmol) of bIm (benzimidazole) were dissolved in 4.8 g of methanol. After that, toluene (4.6 g, 50 mmol), ammonia hydroxide (28–30% aqueous solution, 0.06 g, 1 mmol) and the cobalt acetate dihydrate (0.1250 g, 0.5 mmol) were added to the mix. The solution was stirred at RT for 3 hours.

ZIF-CoNIm (RHO)

5 Batches of ZIF-CoNIm (RHO topology) ($C_6H_4CoN_6O_4$, empirical formula) were successfully synthesized [6]. 0.056 g (0.49 mmol) of 2-nitroimidazole were dissolved in 2.5 mL of DEF, together with 0.072 g (0.24 mmol) of cobalt nitrate ($Co(NO_3)_2 \cdot 6\ H_2O$) in 1.25 mL of DEF. The mix was stirred together in a hydrothermal bomb and heated up to 120 °C to react solvothermally for 14 h.

UiO-66

3 Batches of UiO-66 ($Zr_6O_4(OH)_4(C_8H_6O_4)_6$) were successfully synthesized using a modified literature protocol [7]. 0.053 g (0.227 mmol) of $ZrCl_4$ were mixed with 0.034 (0.227 mmol) of 1,4-benzenedicarboxylic acid in 15 mL of DMF rather than 24.9 g (340 mmol) due to the limited capacity of the teflon liners used for the synthesis (15 mL). The chemicals were stirred in a hotplate at 200 RPMs until the solids had fully dissolved.

UiO-67

2 Batches of UiO-67 [$Zr_6O_4(OH)_4(BPDC)_6$] were successfully synthesized using a modified literature protocol [7, 11]. 0.053 g (0.227 mmol) of $ZrCl_4$ were mixed with 0.0549 (0.227 mmol) of 4.4’-biphenyldicarboxilic acid (BPDC) in 10 mL of DMF rather than 24.9 g (340 mmol) due to the limited capacity of the teflon liners used for the synthesis (15 mL). The chemicals were stirred in a hotplate at 200 RPMs until the solids had fully dissolved. Then, the prepared solutions were placed in hydrothermal bombs and placed in the oven at 120 °C for 24 h.

MIL-101 (Cr)

2 Batches of MIL-101 (Cr) {[$Cr_3OH(H_2O)_2O[O_2C-C_6H_4-(CO_2)]_3 \cdot nH_2O$} were synthesized using the synthesis protocol from Ferey and co-workers' [12]. For each batch, 0.8000 g of chromium nitrate (III) and 0.3300 g of terepthalic acid and 10 mL of deionised water were placed in the teflon-lined autoclave and stirred until dissolved. After that, the hydrothermal bombs were heated at 180 °C in the oven during 8 hours.

NH_2-MIL-101 (Cr)

2 Batches of NH_2-MIL-101 (Cr) {[$Cr_3OH(H_2O)_2O[O_2C-C_6H_3(NH_2)-(CO_2)]_3 \cdot nH_2O$} were synthesized using the protocol from Jiang *et al.* [2]. For each batch, 0.4995 g of chromium nitrate (III) and 0.2260 g of 2-aminotherepthalic acid and 10 mL of deionised water were placed in the teflon-lined autoclave, and stirred until dissolved. After that, the hydrothermal bomb was heated at 130 °C in the oven during 24 hours.

Model fittings

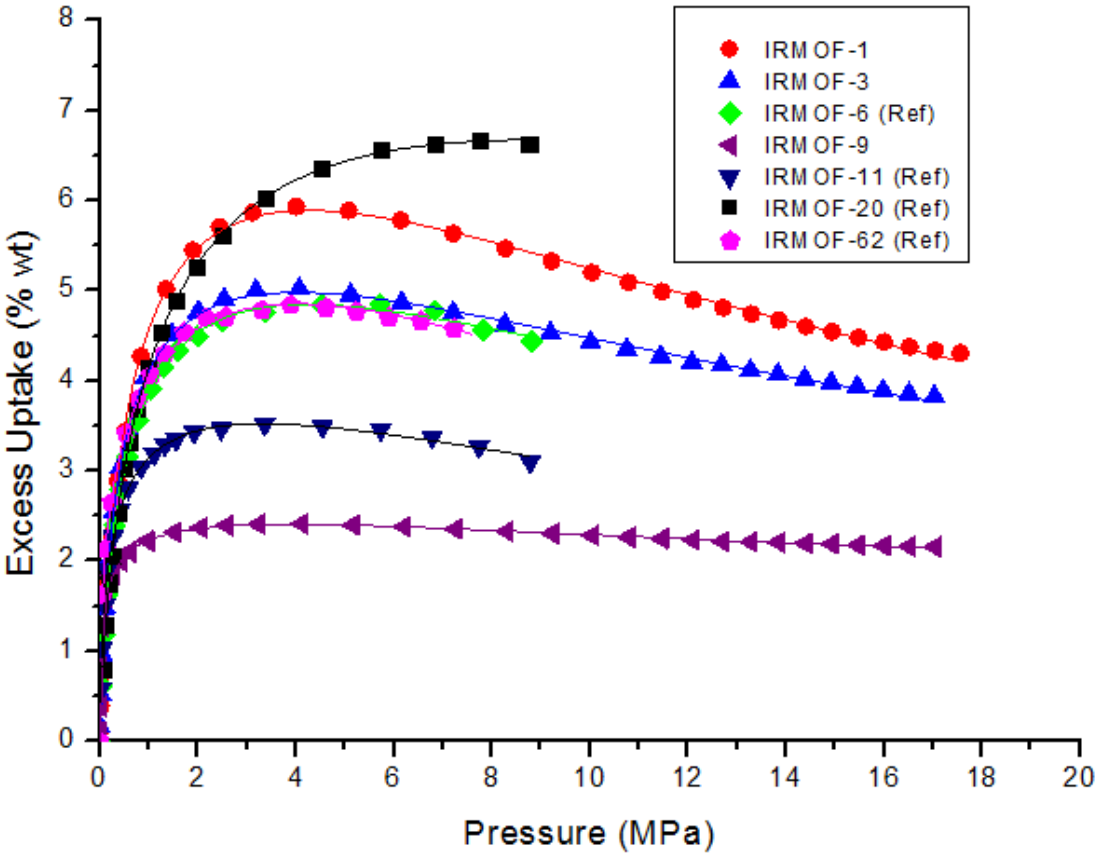

Fig 1. Excess hydrogen isotherms fitting for the IRMOF family of materials at 77 K.

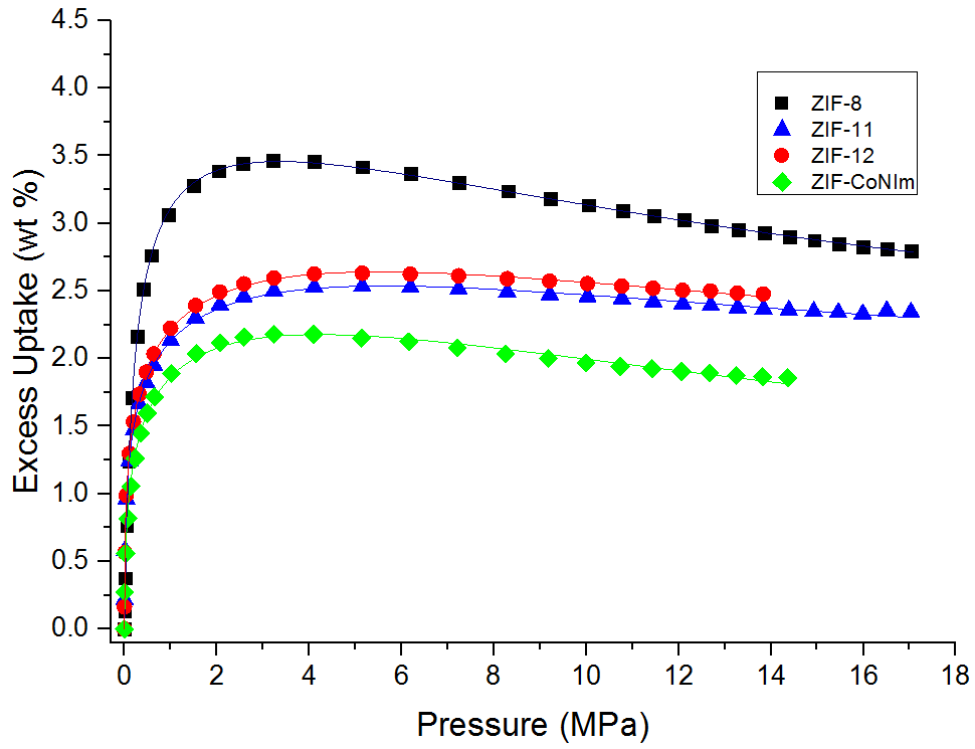

Fig 2. Excess hydrogen isotherms fitting for the ZIF family of materials at 77 K.

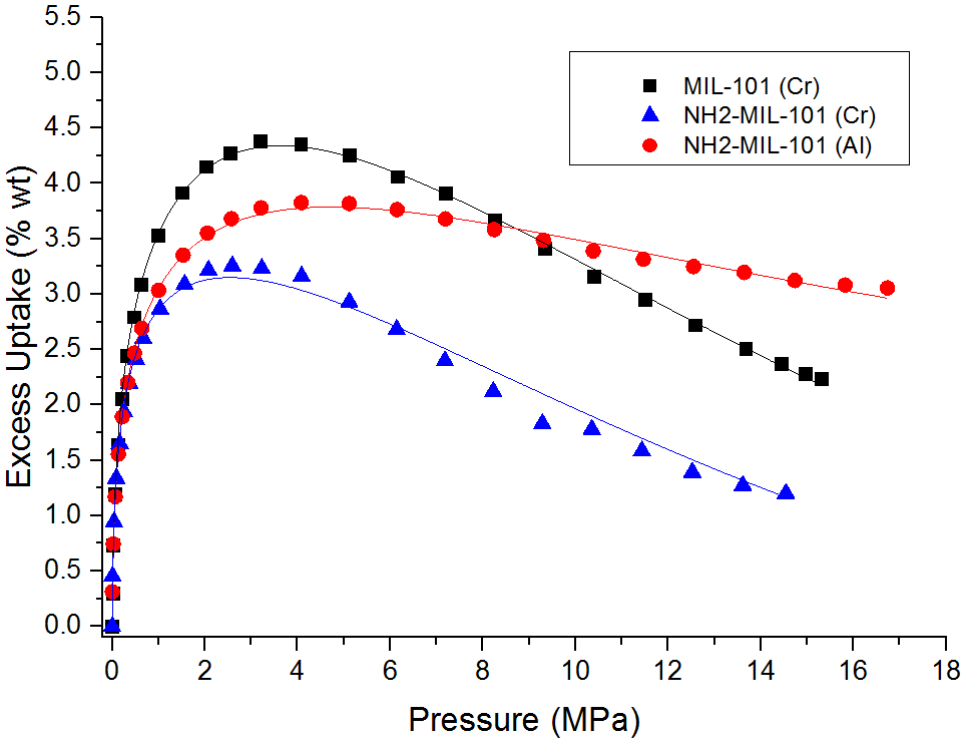

Fig 3. Excess hydrogen isotherms fitting for the MIL family of materials at 77 K.

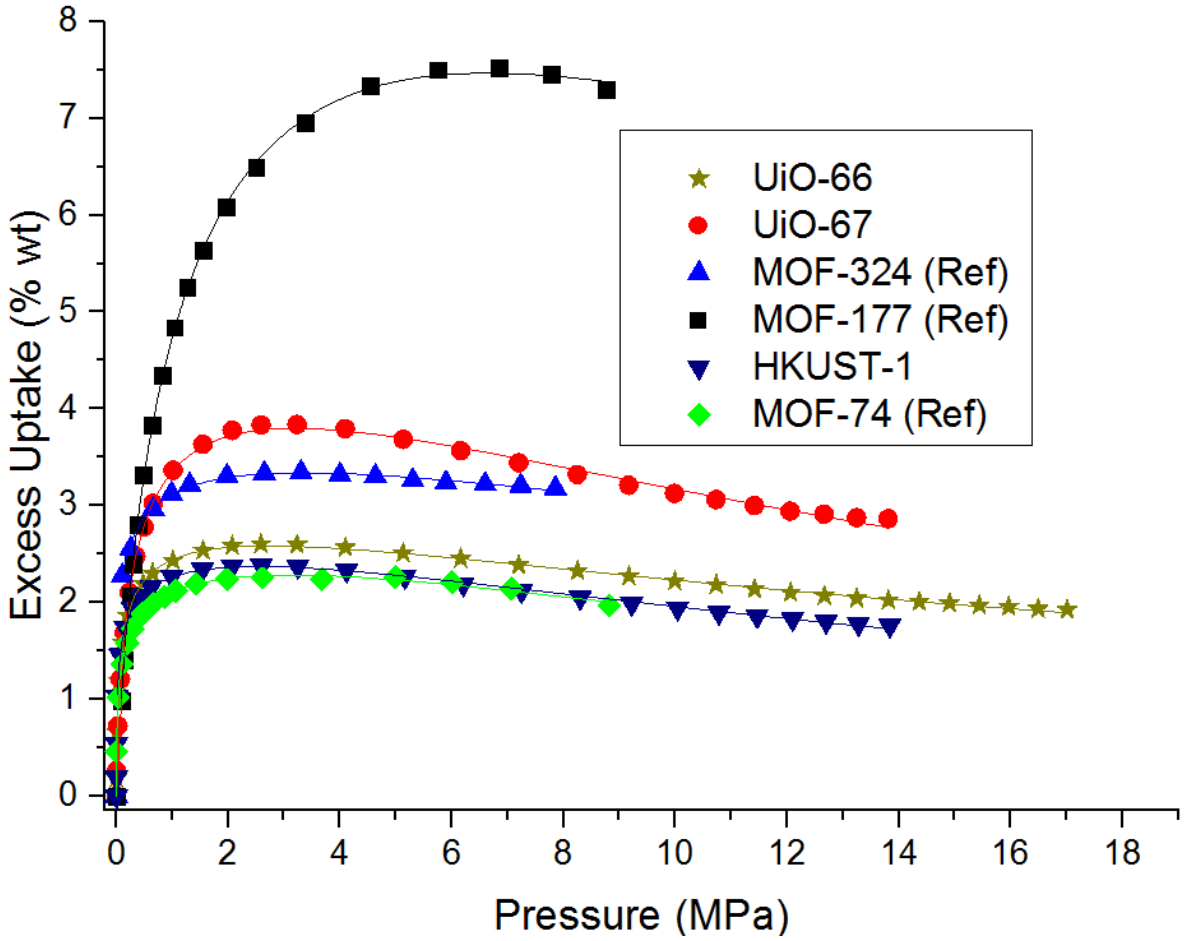

Fig 4. Excess hydrogen isotherms fitting for the UiOs, MOFs and HKUST-1 at 77 K.

UiOs, MOFs and HKUST-1 fitting results.

Total hydrogen data tables

Table 1 shows the total hydrogen values obtained for each material used in the correlation:

Table 1. Total hydrogen quantities.

Material name	Total hydrogen capacity (wt %)	Material name	Total hydrogen capacity (wt %)
IRMOF-1	9.02 ± 0.525	**ZIF-CoNIm**	4.16 ± 0.798
IRMOF-3	7.17 ± 0.419	**NH2-MIL-101 (Cr)**	7.70 ± 1.67
IRMOF-6	7.40 ± 1.22	**NH2-MIL-101 (Al)**	9.23 ± 1.45
IRMOF-9	3.16 ± 0.120	**UiO-66**	3.41 ± 0.118
IRMOF-11	5.07 ± 0.626	**UiO-67**	5.46 ± 0.440
IRMOF-20	8.22 ± 1.35	**MOF-74**	6.04 ± 12.0
ZIF-8	4.17 ± 0.119	**MOF-177**	13.51 ± 3.14
ZIF-11	5.24 ± 0.578	**MOF-324**	6.37 ± 3.10
ZIF-12	5.75 ± 0.568	**HKUST-1**	3.84 ± 0.490

Data summary table

Table 2 summarizes all the characterization data obtained from nitrogen sorption experiments and literature. BET_1 values from the first row of each material were used in the correlations, adding literature values in the following row/s. BET_2 values were calculated using the standard 5 point BET test (0.05-0.3 P/Po) so data could be easily compared with literature. More literature data was gathered in order to compare with experiments and different literature publications:

Table 2. Summary of properties (BET, pore volume and pore diameter) for the different MOFs used.

MOF	BET_1 Surface area ($m^2 g^{-1}$)	Methodology /Reference	BET_2 Surface area ($m^2 g^{-1}$)	Methodology/ Reference	Pore Volume ($cm^3 g^{-1}$)	Methodology/ Reference	Pore Diameter (nm)	Methodology /Reference
IRMOF-1	3444 ± 16	From 4.8E-6 to 0.034 P/Po. N_2 at 77K. R^2=0.9999	2703 ± 127	From 0.05 to 0.3 P/Po. N_2 at 77K. R^2=0.9958	1.38 0.50	N_2 isotherm, total HK method at 0.99 P/Po N_2 isotherm, DR method	1.3	DFT, slit pore N_2. SDF: 1.85 E-2 mmol g^{-1}
	3534	From 0.02 to 0.1 P/Po. N_2 at 77K [13]	-	-	1.13 1.186	N_2 isotherm, Gurvitch method [14] MOFormics (software) [15]	1.21 and 1.50 1.215	X-Ray [16] X-Ray [14]
IRMOF-3	1728 ± 14	From 1.23E-5 to 0.046 P/Po. N2 at 77K. R2=0.9999	1234 ± 75	From 0.05 to 0.3 P/Po. N_2 at 77K. R^2=0.9949	0.66 0.68	N_2 isotherm Total HK method at 0.99 P/Po N_2 isotherm, DR method	1.2	DFT, slit pore N_2. SDF: 0.72 mmol g^{-1}
	2163 and 2120	No ranges stated [17]	-	-			Around 4	(BJH) [18]
IRMOF-6	2804	From 0.02 to 0.1 P/Po. N_2 at 77K [13]	-	-	0.993 1.14	N_2 isotherm, Gurvitch method [14] N_2 isotherm, DR method	0.97 and 1.5	X-Ray [16]

						[16]		
	2476	BET, methodology not stated. N_2 at 77K [16]						
IRMOF-9	1444 ± 14	From 8.52E-7 to 0.049 P/Po. N_2 at 77K. R^2=0.9998	1118 ± 54	-	0.59 0.72	N_2 isotherm, total HK method at 0.99 P/Po N_2 isotherm, DR method	1.2	DFT, slit pore N_2. SDF: 0.15 mmol g^{-1}
							1.45	Cerius2 (1.06 nm pore aperture) [19]
IRMOF-11	1984	From 0.02 to 0.1 P/Po. N_2 at 77K [13]	-	-	0.830	N_2 isotherm, Gurvitch method [14]	1.58	X-Ray [19]
IRMOF-20	4024	From 0.02 to 0.1 P/Po. N_2 at 77K [13]	-	-	1.53	N_2 isotherm, DR method [14]	1.4 and 1.73	X-Ray [16]
	4593	From 0.02 to 0.35 P/Po. N_2 at 77K [13]	3409	BET, methodology not stated. N_2 at 77K [16]				
IRMOF-62	2420	[20]	-	-	0.91	N_2 isotherm, DR method [20]	0.52	Cerius2 [20]
	2550	[21]						
MOF-74	950	From 0.02 to 0.1 P/Po. N_2 at 77K [4]	1072	From 0.02 to 0.35 P/Po. N_2 at 77K [4]	0.327	N_2 isotherm, Gurvitch method [10]	1.1	[14] X-Ray
MOF-177	4746	From 0.02 to 0.1 P/Po. N_2 at 77K [13]	4730	From 0.03 to 0.07 P/Po. N_2 at 77K [22]	2.65 1.75	N_2 isotherm, total HK method [23]	1.117 1.06	[14] X-Ray [24] N_2 isotherm

						N_2 isotherm, Gurvitch method [14]		
MOF-324	1600	[20]	-	-	0.59	N_2 isotherm, DR method [20]	0.76	[20] Cerius2
NH_2-MIL-101 (Al)	2543 ± 63	From 0.05 to 0.3 P/Po. N_2 at 77K. R^2=0.9973	-	-	0.77	N_2 isotherm, DR method. Lab data	1.2 and 1.6	Lab data
	2100	From 0.05 to 0.15 P/Po. N_2 at 77K [8].						
NH_2-MIL-101 Cr	1632 ± 33	From 1.1E-5 to 0.19 P/Po. N_2 at 77K. R^2=0.9993	1515 ± 66	From 0.05 to 0.3 P/Po. N_2 at 77K. R^2=0.9973	1.35 0.55	N_2 isotherm Total HK method at 0.99 P/Po N_2 isotherm, DR method	1.2 and 1.6 1.3, 1.5, 2.0 and 2.5	BJH. Experimental data DFT, slit pore N_2. SDF: 0.17 mmol g^{-1}
	2070	From 0.05 to 0.1 P/Po. N_2 at 77K. [2]			2.26	N_2 isotherm, total pore volume at 0.99 P/Po [2]	1.54 and 1.99	[2] BJH
MIL-101 Cr	2555 ± 71	From 3.3E-6 to 0.25 P/Po. N_2 at 77K. R^2=0.9988	2456 ± 117	From 0.05 to 0.3 P/Po. N_2 at 77K. R^2=0.9967	1.78 0.81	N_2 isotherm, total HK method at 0.99 P/Po N_2 isotherm, DR method	1.2 and 1.6 1.3, 2.2 and 2.7	BJH. Experimental data DFT, slit pore N_2. SDF: 0.30 mmol g^{-1}

	2944	From 0.05 to 0.1 P/Po. N_2 at 77K. [25]	2761	From 0.01 to 0.12 P/Po. N2 at 77K. [26]	2.57 1.51	N_2 isotherm, total pore volume at 0.99 P/Po [25] N_2 isotherm, Gurvitch method at 0.95 P/Po [26]	1.6 and 2.1 0.7, 2.9 and 3.4 1.3 and 2.16	[25] BJH [26] Model data [27] DFT
ZIF-7	1676	Cerius2, single crystal x-ray [28]	1676	Cerius2, single crystal x-ray [28]	0.582	Cerius2, single crystal x-ray [28]	1.46	Cerius2, single crystal x-ray [28]
ZIF-8	1842 ± 68	From 1.13E-5 to 0.024 P/Po. N2 at 77K. R2=0.9979	1306 ± 63	From 0.05 to 0.3 P/Po. N_2 at 77K. R2=0.9968	1.63 0.68	N_2 isotherm, total HK method at 0.99 P/Po N_2 isotherm, DR method	1.2	DFT, slit pore N_2. SDF: 0.78 mmol g^{-1}
	962	From 9E-3 to 8.4E-2 P/Po. N_2 at 77K. R2=0.9996 [5]			0.36	N_2 isotherm, micropore volume (method not stated) at P/P0 = 3.3E-2 [5]		
	1025	N_2 isotherm [29]	-	-	0.75 total 0.61 micro	N_2 isotherm, total pore volume [29] N_2 isotherm, microporous volume [29]	0.352 and 4.43	N_2 isotherm (methodology not stated) [29]
	1947	Cerius2, single crystal x-ray [28]	1947	Cerius2, single crystal x-ray [28]	0.663	Cerius2, single crystal x-ray [28]	11.6	Cerius2, single crystal x-ray [28]

ZIF-9	1428	N_2 isotherm [30]	-	-	0.12	Single crystal XRD and software that evaluates volume accessible to He (using modified UFF parameters from paper) [28, 31]	0.431	Methodology not stated [30]
ZIF-11	1676	Cerius2, single crystal x-ray [28]	1676	Cerius2, single crystal x-ray [28]	0.582	Cerius2, single crystal x-ray [28]	1.46	Cerius2, single crystal x-ray [28]
					0.457	PLATON software [32]	1.49	PLATON software [32]
ZIF-12	926	From 2.5E-3 to 0.022 P/Po. N2 at 77K. R^2=0.9974	727	From 0.05 to 0.3 P/Po. N_2 at 77K. R^2=0.9957	0.54 0.39	N_2 isotherm, Gurvitch method at 0.985 P/Po N_2 isotherm, DR method	0.66 and 1.4	HK for spherical pores
CoNIm (RHO)	1405 ± 40	From 6.62E-7 to 0.047 P/Po. N_2 at 77K. R^2=0.9988	1015 ± 64	From 0.05 to 0.3 P/Po. N_2 at 77K. R2=0.9946	0.53 0.63	N_2 isotherm Total HK method at 0.99 P/Po N_2 isotherm, DR method	1.2 and 1.5 1.2	DFT, cylinderpores in pillared clay. SDF: 0.44 mmol g^{-1} DFT, slit pore N_2. SDF: 0.48 mmol g^{-1}
	1858	BET. Range	-	-	0.827	N_2 isotherm,	2.23	X-ray single

		not stated. N_2 isotherm [6]				micropore volume at P/Po = 0.1 [6]		cristal [6]
UiO-66	823 ± 42	From 3.77E-7 to 0.032 P/Po. N2 at 77K. R^2=0.9963	870 ± 25	From 0.05 to 0.3 P/Po. N_2 at 77K. R2=0.9977	0.50 0.44	N_2 isotherm, total HK method at 0.99 P/Po N_2 isotherm, DR method	0.68 and 0.85 0.6 and 0.77	DFT, slit pore N_2. SDF: 0.24 mmol g^{-1} DFT, cylinder Tarazona NLDFT. SDF: 0.43 mmol g^{-1}
	969	From 0.05 to 0.25 P/Po. N_2 at 77K [33]	-	-	0.52 0.43	N_2 isotherm. Total pore volume at P/Po = 0.97 Micropore pore volume, T-plot (Harkins and Jura equation) [33]	0.75 and 1.2	DFT, cylinder Tarazona NLDFT [33].
UiO-67	1351 ± 40	From 4.3E-7 to 0.035 P/Po. N2 at 77K. R^2=0.9965	1261 ± 62	From 0.05 to 0.3 P/Po. N_2 at 77K. R2=0.9966	0.78 0.67	N_2 isotherm Total HK method at 0.99 P/Po N_2 isotherm, DR method	1.1 0.62 and 1.0	DFT, slit pore N_2. SDF: 0.50 mmol g^{-1} DFT, cylinder Tarazona NLDFT. SDF: 0.65 mmol g^{-1}
	1877	From 0.05 to 0.25 P/Po. N_2 at 77K [33]	-	-	0.95	N_2 isotherm, total pore volume at	1.2 and 1.6	DFT, cylinder Tarazona NLDFT [33].

					0.85	P/Po = 0.97 Micropore pore volume, T-plot (Harkins and Jura equation) [33]		
HKUST-1	1343 ± 82	From 7.67E-7 to 0.013 P/Po. N_2 at 77K. R^2=0.9949	1822 ± 4	From 0.05 to 0.3 P/Po. N_2 at 77K. R^2=0.9999	0.71 0.67	N_2 isotherm, total HK method at 0.99 P/Po N_2 isotherm, DR method	0.46 and 0.85	DFT, slit pore N_2. SDF: 0.45 mmol g^{-1}
	1507	BET, methodology not stated. N2 at 77K [16]	1645	Methodology not stated [34]	0.833 0.804	N_2 isotherm, total pore volume [34] N_2 isotherm, DR method [34]	0.57 and 1.1	DFT (desorption) [34]

X-Ray Diffraction figures

X-ray tests were compared with the original CIF files obtained from the Cambridge Crystallographic database. When tests did not fully match with the CIFs or to get extra synthesis confirmation, data was compared with experimental data from literature for comparison, ensuring the materials were synthesized successfully. The literature used to compare will be included in the legend of the figure. For ZIFs 7 to 12, data was also double checked by the publication authors.

IRMOF-1

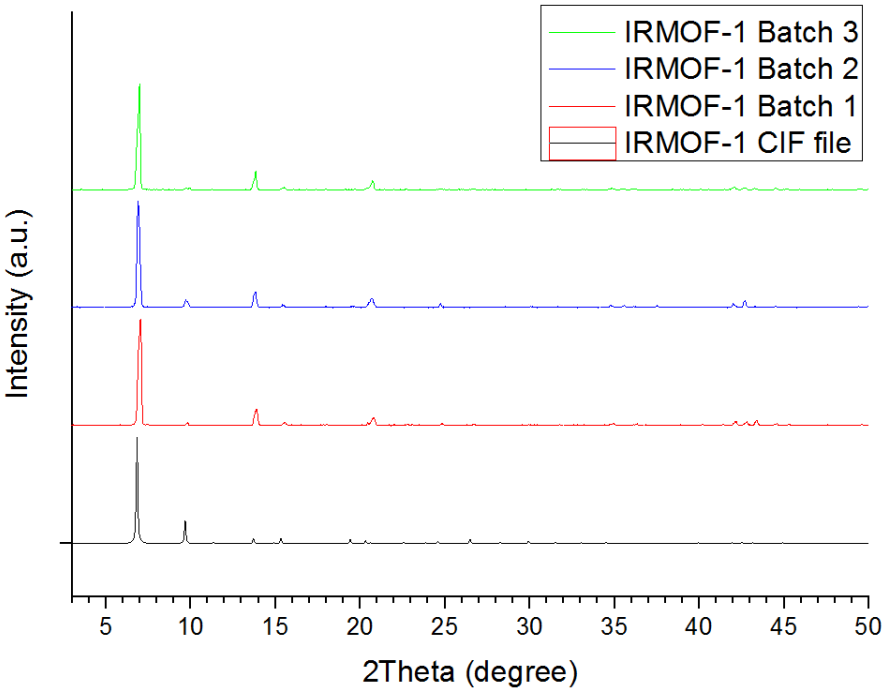

Fig 5. PXRD of IRMOF-1. PXRD from CIF file (black) and results from three synthesized batches (red, blue and green) [14].

IRMOF-3

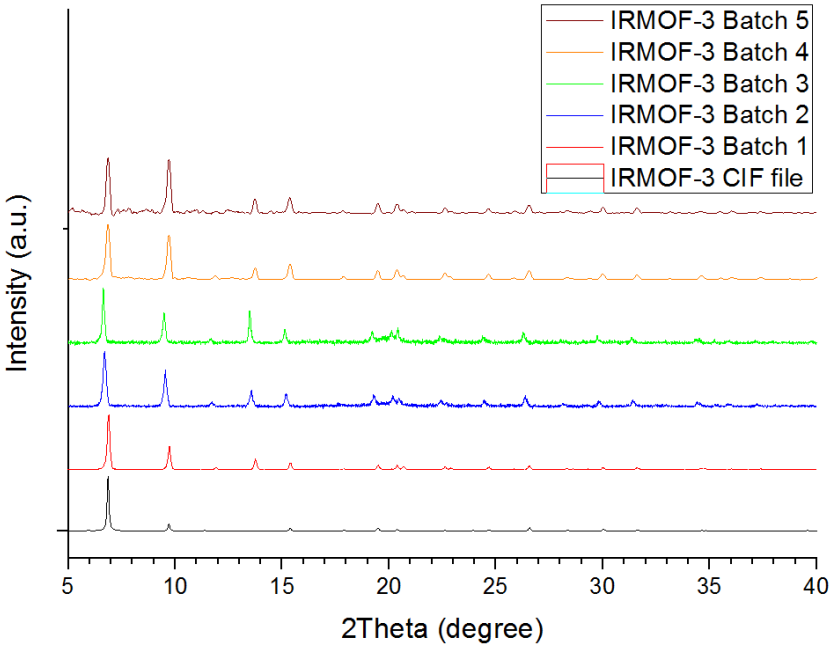

Fig 6. PXRD of IRMOF-3. PXRD from CIF file (black) and results from the five synthesized batches (red, blue, green, orange and brown) [35].

IRMOF-8

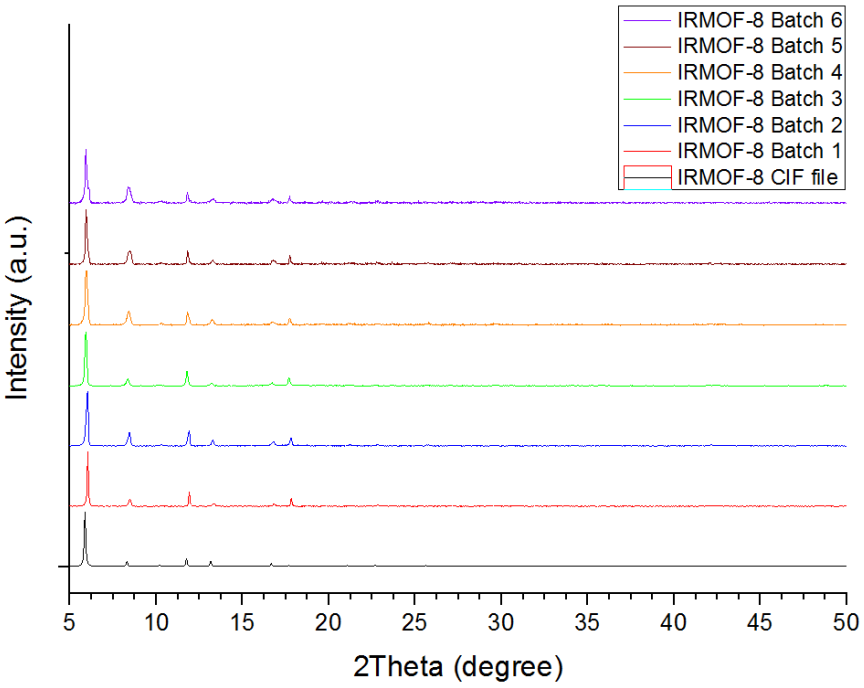

Fig 7. PXRD of IRMOF-8. PXRD from CIF file (black) and results from the six synthesized batches (red, blue, green, orange, brown and purple) [36].

IRMOF-9

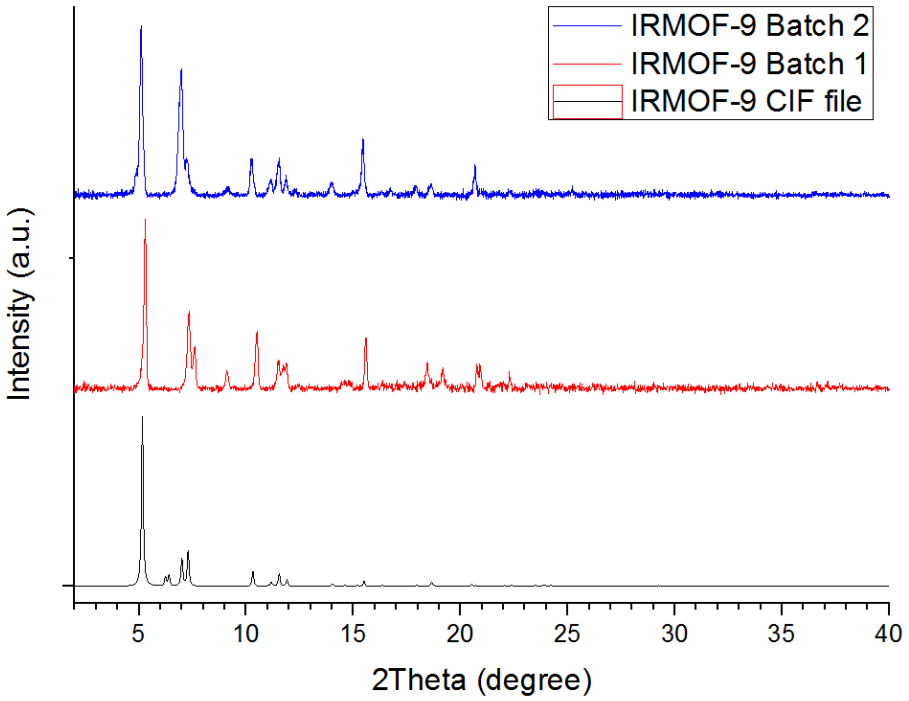

Fig 8. PXRD of IRMOF-9. PXRD from CIF file (black) and results from the two synthesized batches (red and blue) [3].

ZIF-7

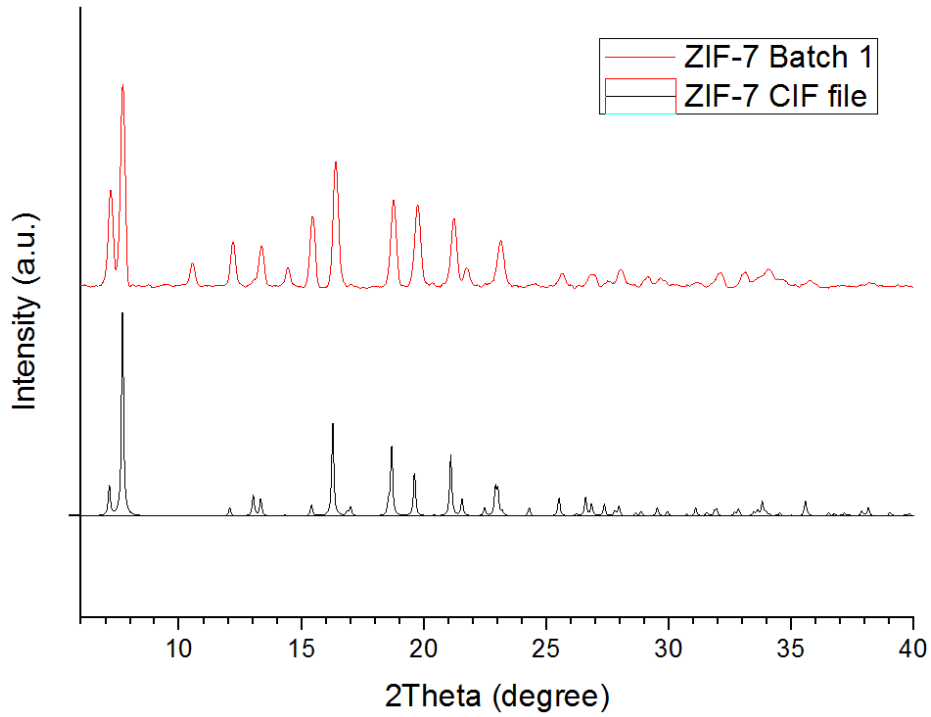

Fig 9. PXRD of ZIF-7. PXRD from CIF file (black) and the synthesized batch [4].

ZIF-8

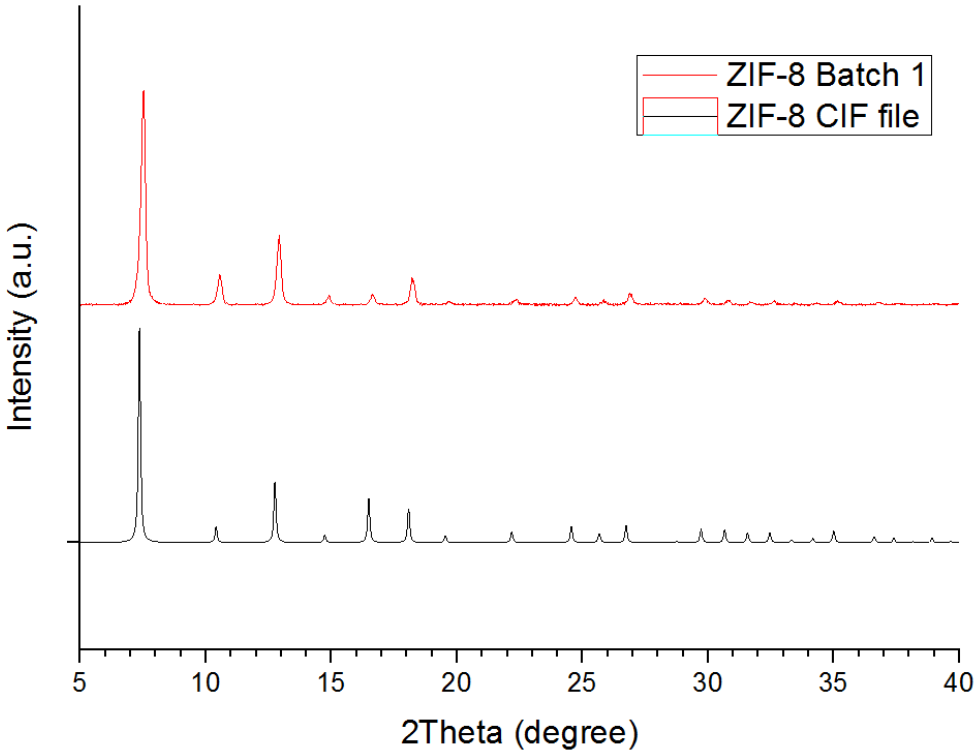

Fig 10. PXRD of ZIF-8. PXRD from CIF file (black) and results from the synthesized batch (red) [37].

ZIF-9

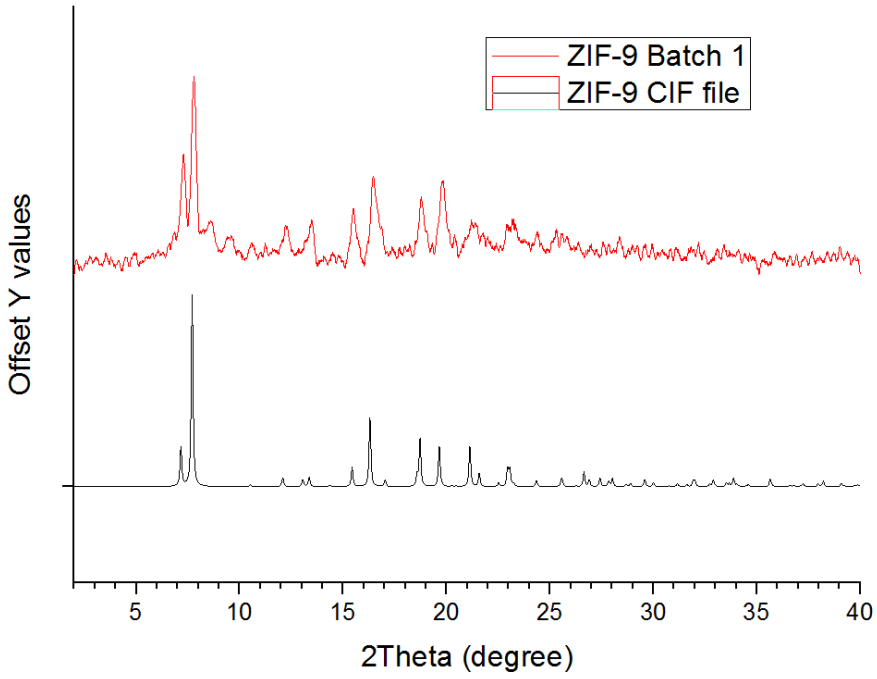

Fig 11. PXRD of ZIF-9. PXRD from CIF file (black) and results from the synthesized batch [30].

After discussing with the authors and an expert from the University of Bath, it was determined to be a minor structural change because the initial solvent where the sample was evaporated using a vacuum oven at room temperature whereas the authors left it evaporate at room temperature and pressure.

ZIF-11

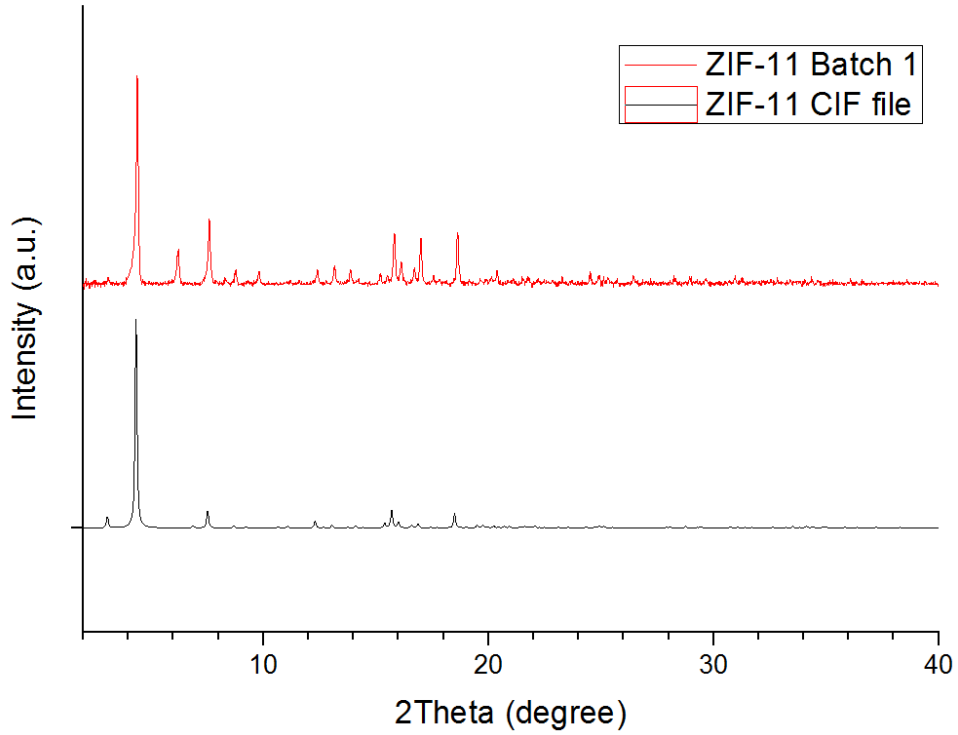

Fig 12. PXRD of ZIF-11. PXRD from CIF file (black) and results from the synthesized batch [4].

ZIF-12

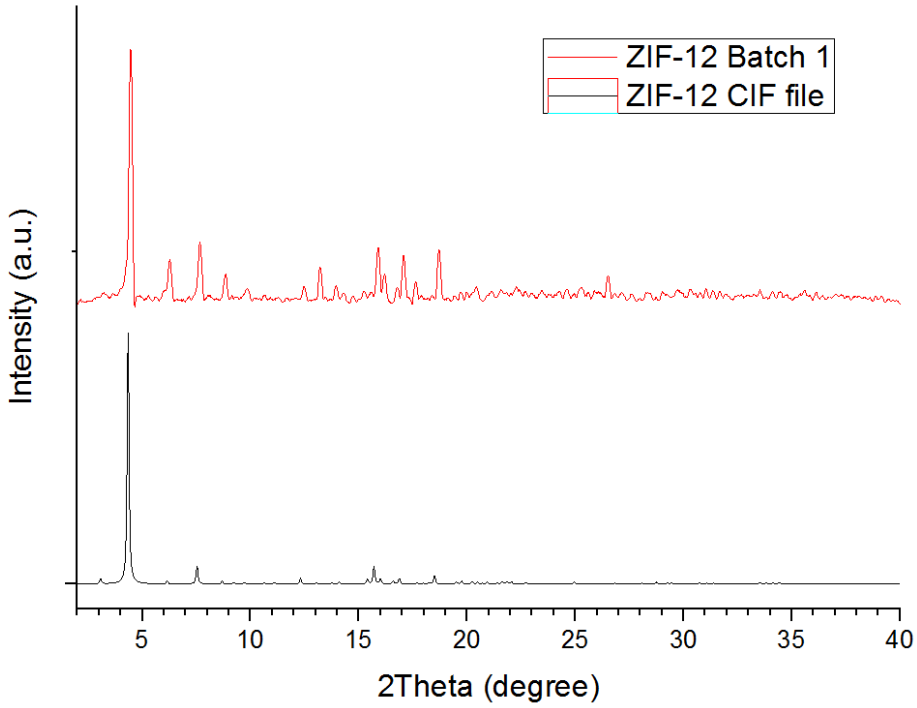

Fig 13. PXRD of ZIF-12. PXRD from CIF file (black) and results from the synthesized batch (red) [4].

CoNIm (RHO)

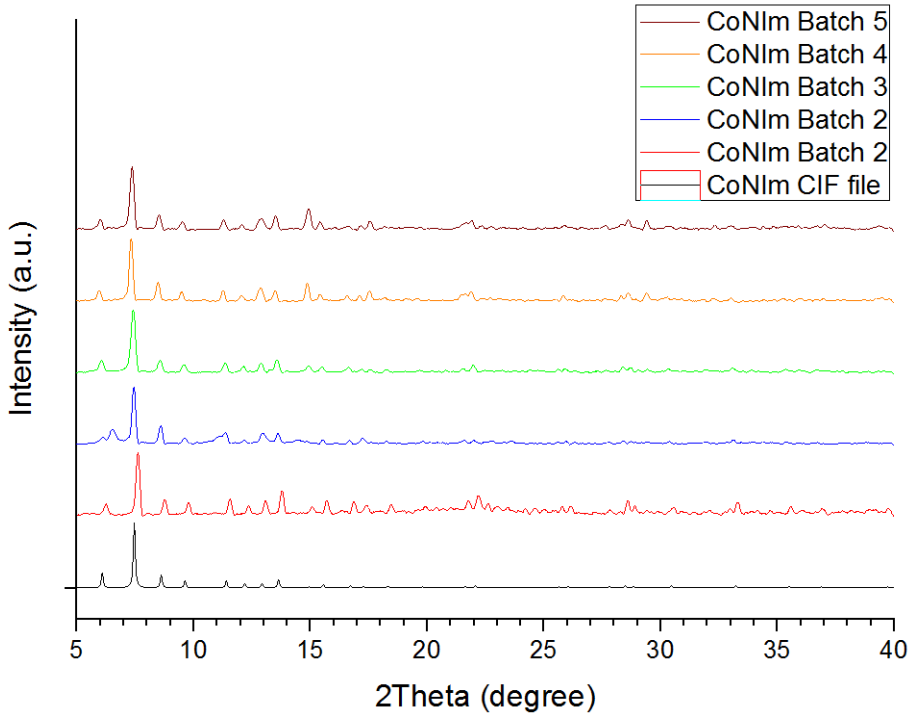

Fig 14. XRD patterns of CoNIm (RHO). CIF file (black), evacuated batches, 1 to 5 [6].

MIL-101 (Cr)

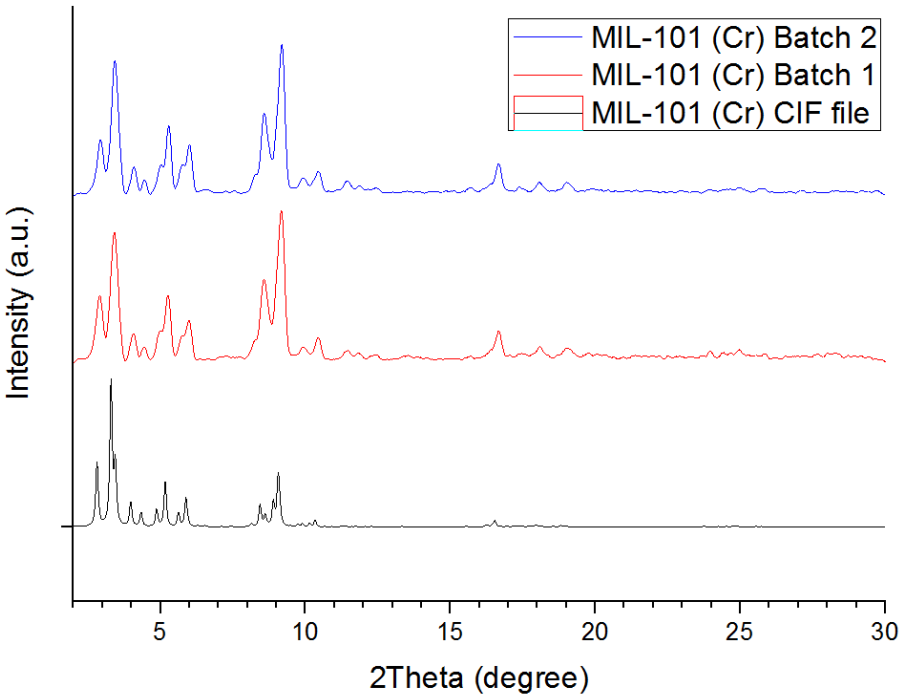

Fig 15. XRD patterns of MIL-101 (Cr). CIF file (black) and experimental batches 1 and 2 (red and blue) [38].

NH_2-MIL-101 (Cr)

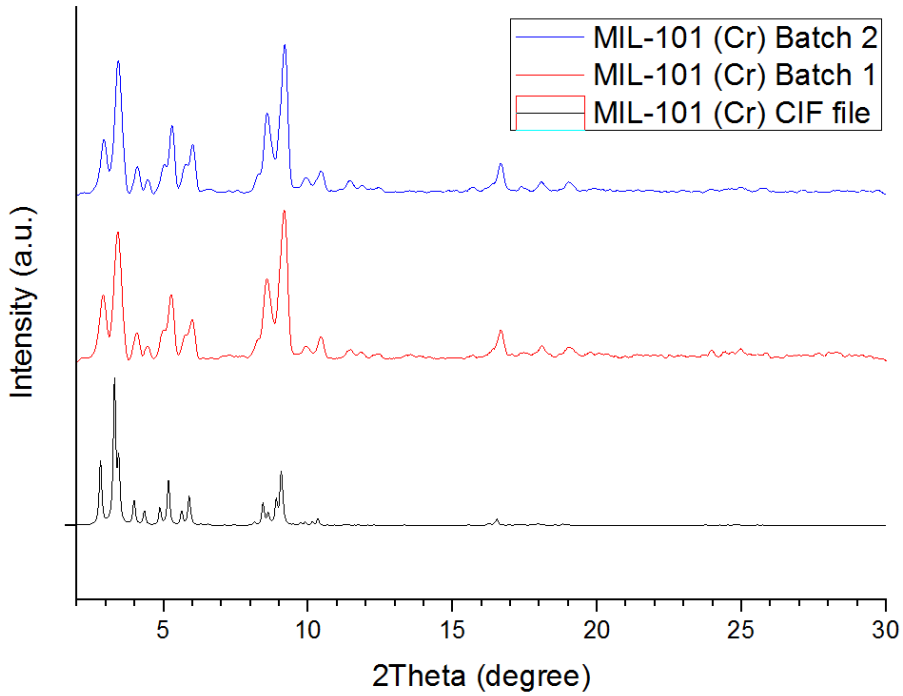

Fig 16. XRD patterns of NH_2-MIL-101 (Cr). CIF file of MIL-101 (Cr) (black) and experimental NH_2-MIL-101 (Cr) batches 1 and 2 (red and blue).

No CIF file was found for NH_2-MIL-101 (Cr) in the crystallography database. Given that NH_2-MIL-101 (Cr) and MIL-101 (Cr) have the same framework and the X-ray scattering will be dominated by the metal centres, the powder patterns will be virtually identical, especially given that the amino groups will be disordered. The same approach has been seen in literature [2].

NH_2-MIL-101 (Al)

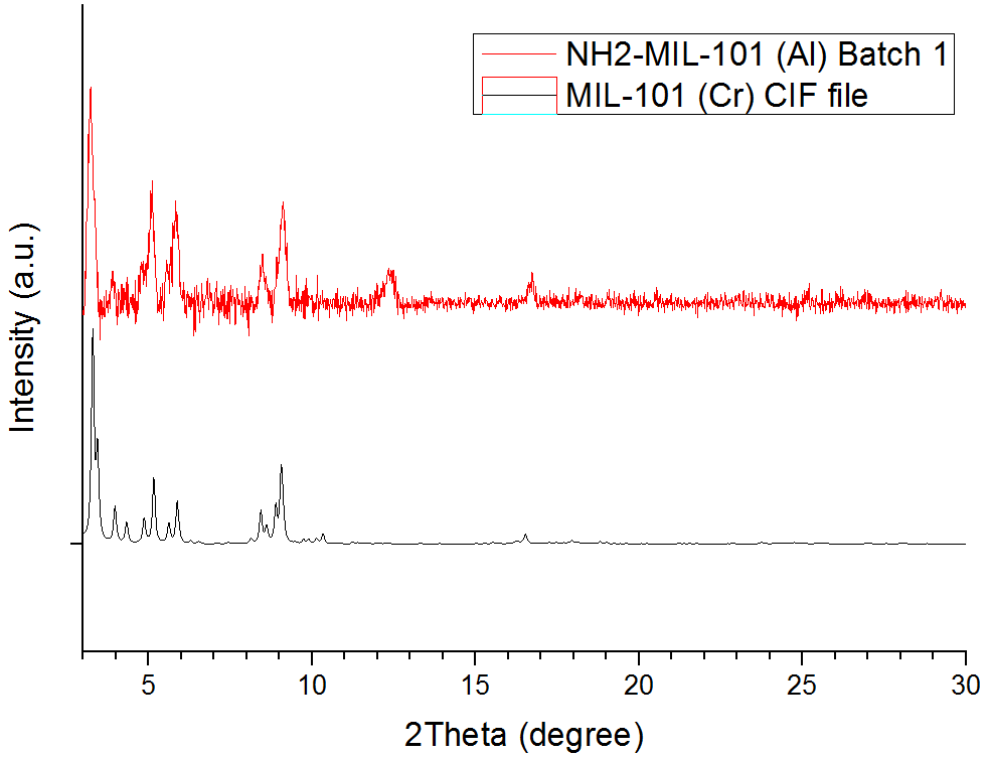

Fig 17. XRD pattern of NH_2-MIL-101 (Al). CIF file of MIL-101 (Cr) (black) and experimental NH_2-MIL-101 (Al) batch (red), compared as in literature [8].

UiO-66

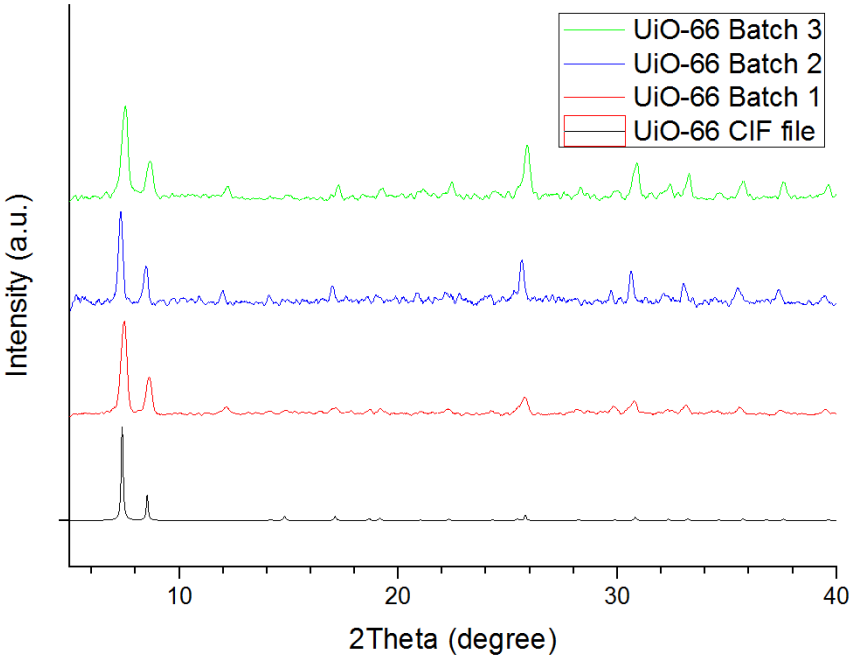

Fig 18. XRD patterns of UiO-66. CIF file (black), batches following the hydrothermal bomb methodology (red, blue and green). Extra peak at 12 2θ is caused by the presence of water in the pores.

UiO-67

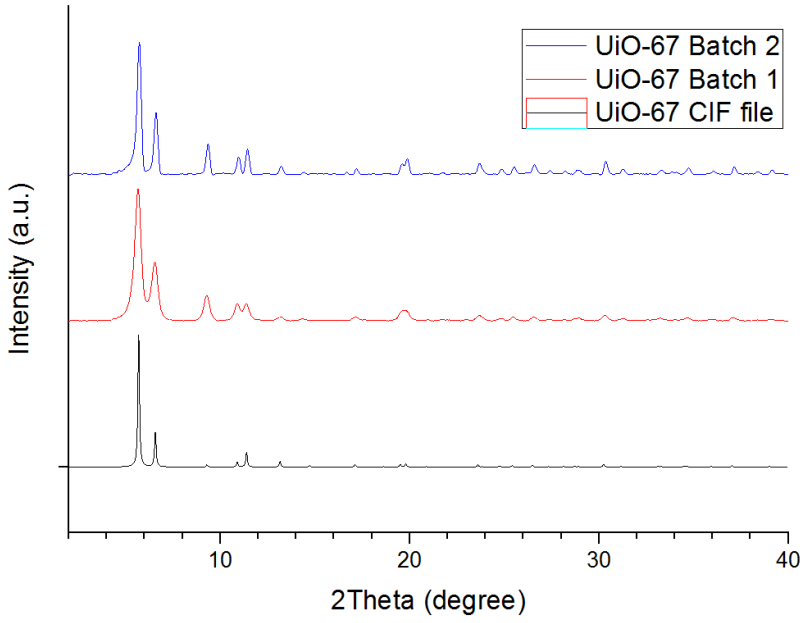

Fig 19. XRD patterns of UiO-67. CIF file (black), and experimental batches (red and blue) [33].

HKUST-1

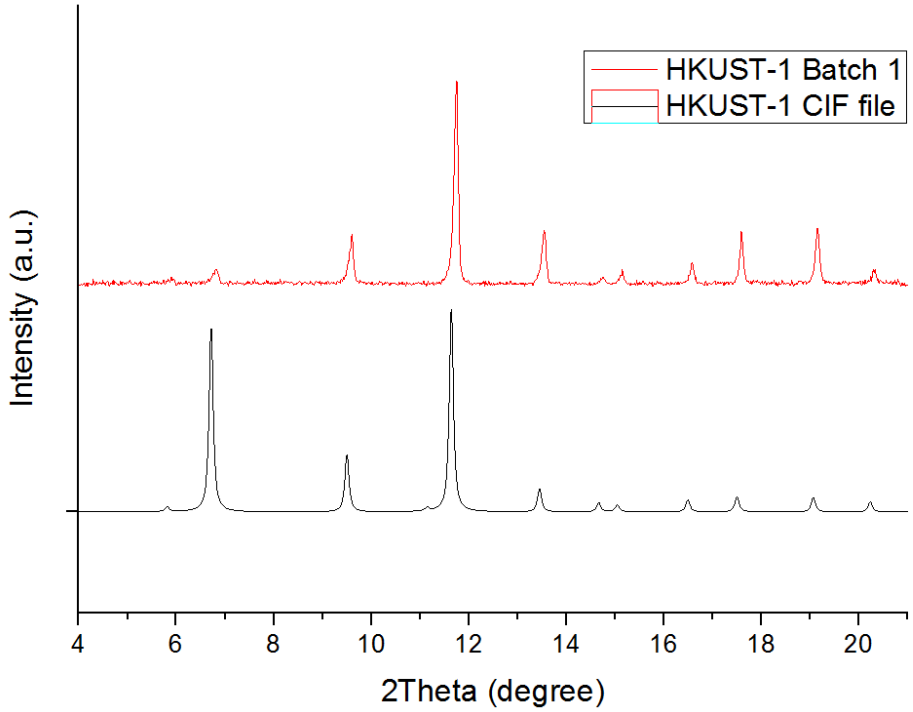

Fig 20. XRD patterns of HKUST-1. CIF file (black), commercial sample (red) [39].

4.1 Thermogravimetric analyser results

Table 3. Degassing conditions chosen for every material from TGA data.

Material	Degassing temperature (°C)
IRMOF-1	225
IRMOF-3	200 [40]
IRMOF-8	200 [41]
IRMOF-9	200
ZIF-7	200
ZIF-8	200
ZIF-9	225
ZIF-11	250
ZIF-12	300
CoNIm (RHO)	200 [6]
MIL-101 (Cr)	180
NH_2-MIL-101 (Cr)	180
UiO-66	300
UiO-67	300
HKUST-1	250 [39]

IRMOF-1

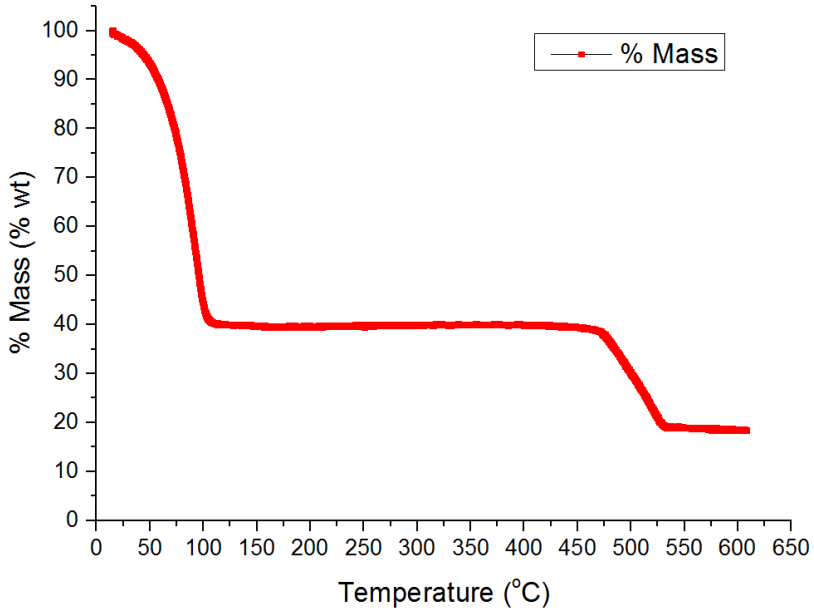

Fig 21. IRMOF-1 TGA test from 20 to 600 °C, 5 °C min^{-1} under nitrogen.

IRMOF-3

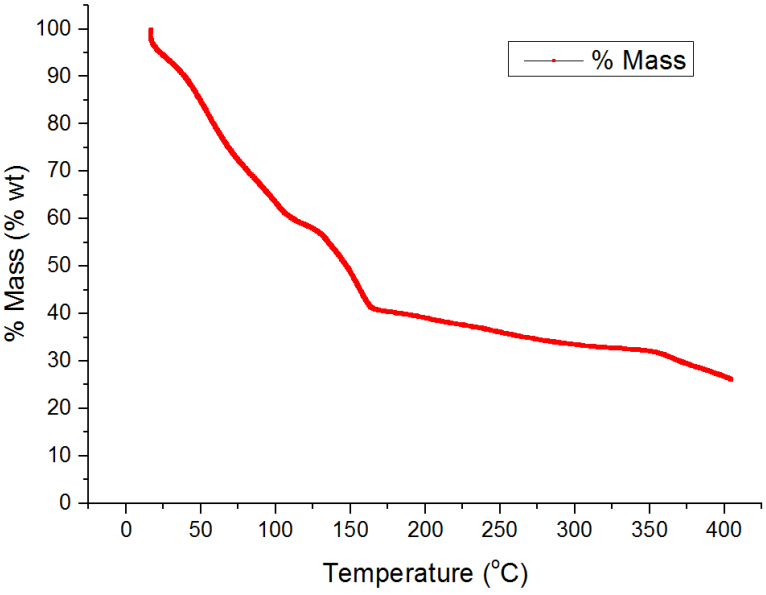

Fig 22. IRMOF-3 TGA test from 20 to 400 °C, 5 °C min^{-1} under nitrogen. Checked with literature [40].

IRMOF-9

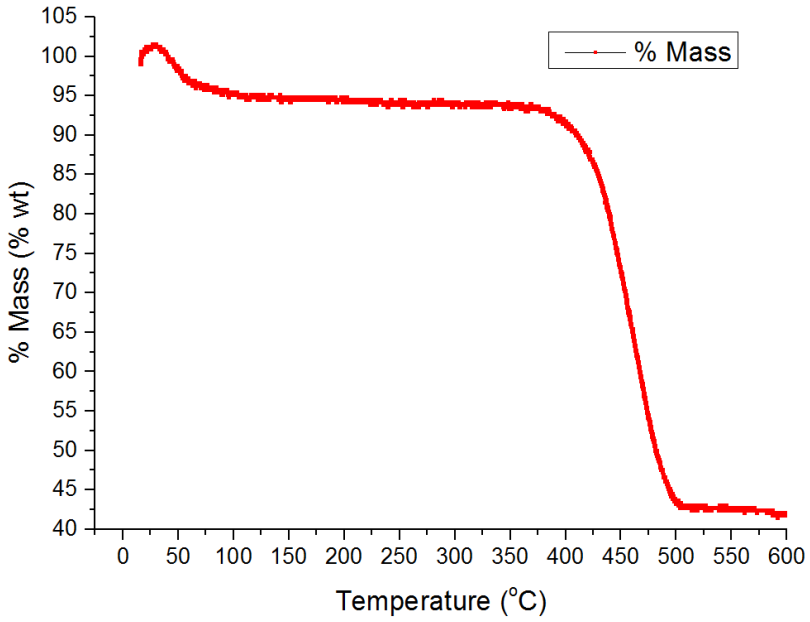

Fig 23. IRMOF-9 B1 TGA test from 20 to 600 °C, 5 °C min^{-1} under nitrogen.

ZIF-7

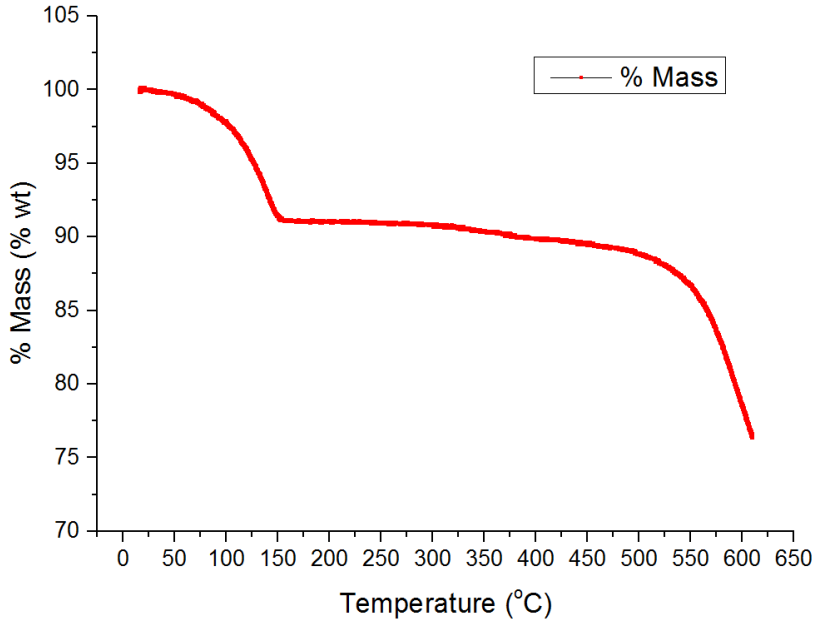

Fig 24. ZIF-7 TGA test from 20 to 600 °C, 5 °C min^{-1} under nitrogen.

ZIF-8

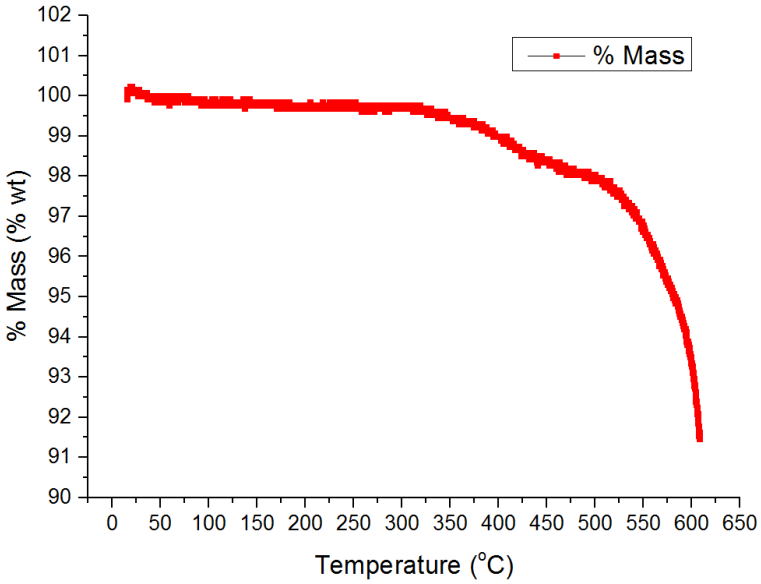

Fig 25. ZIF-8 TGA test from 20 to 600 °C, 5 °C min^{-1} under nitrogen.

ZIF-9

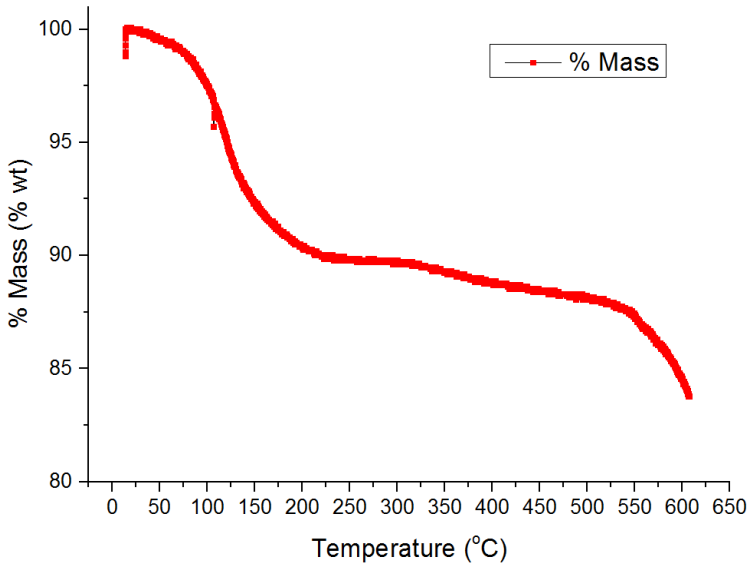

Fig 26. ZIF-9 TGA test from 20 to 600 °C, 5 °C min^{-1} under nitrogen.

ZIF-11

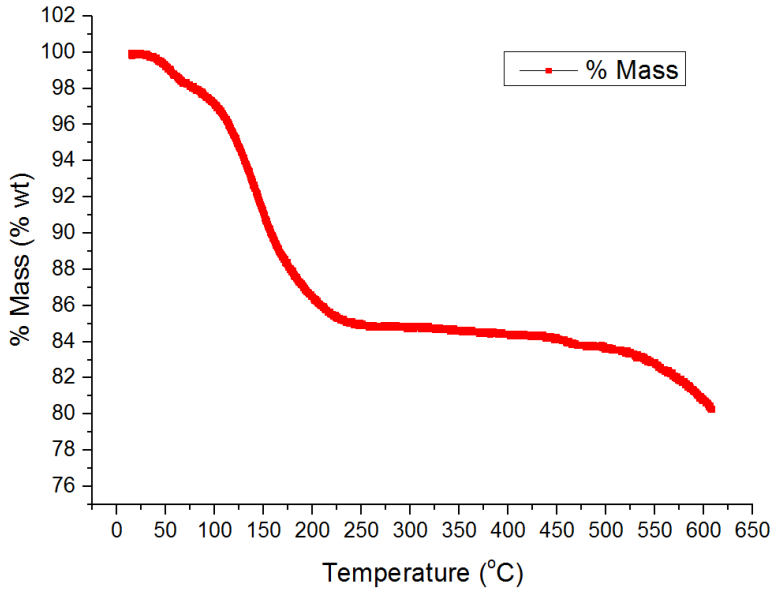

Fig 27. ZIF-11 TGA test from 20 to 600 °C, 5 °C min^{-1} under nitrogen.

ZIF-12

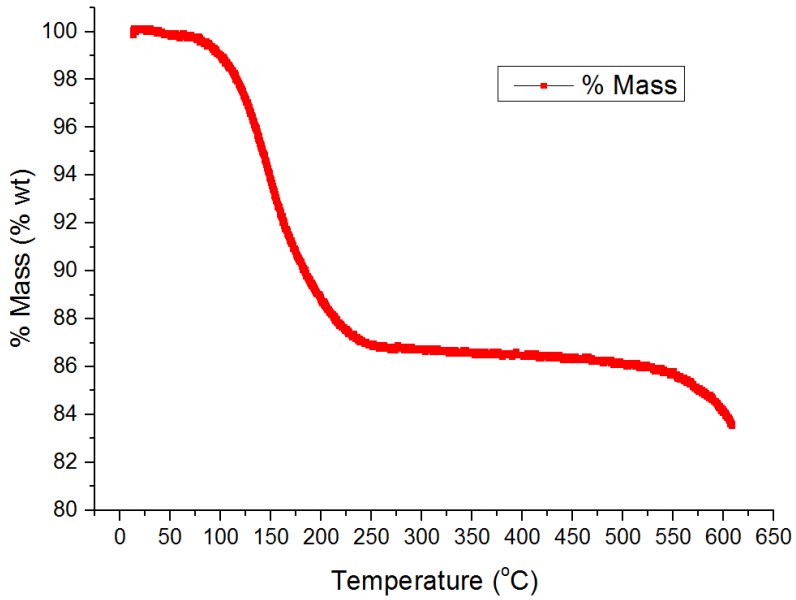

Fig 28. ZIF-12 TGA test from 20 to 600 °C, 5 °C min^{-1} under nitrogen.

MIL-101 (Cr)

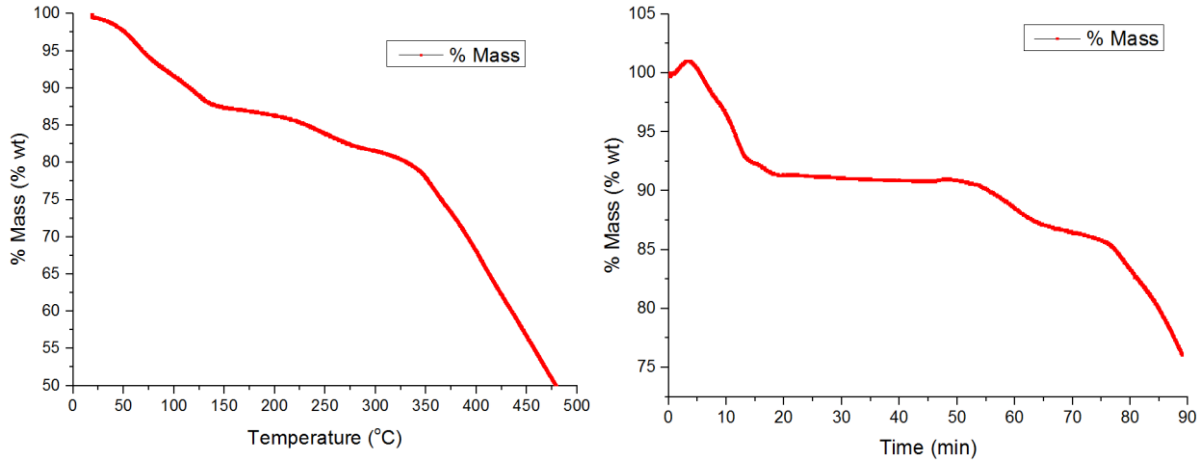

Fig 29 and 30. MIL-101 (Cr) TGA test from 20 to 600 °C and test from 20 to 450 °C, holding temperature at 180 °C for 30 minutes, 5 °C min^{-1} under nitrogen. Checked with literature [1].

NH_2-MIL-101 (Cr)

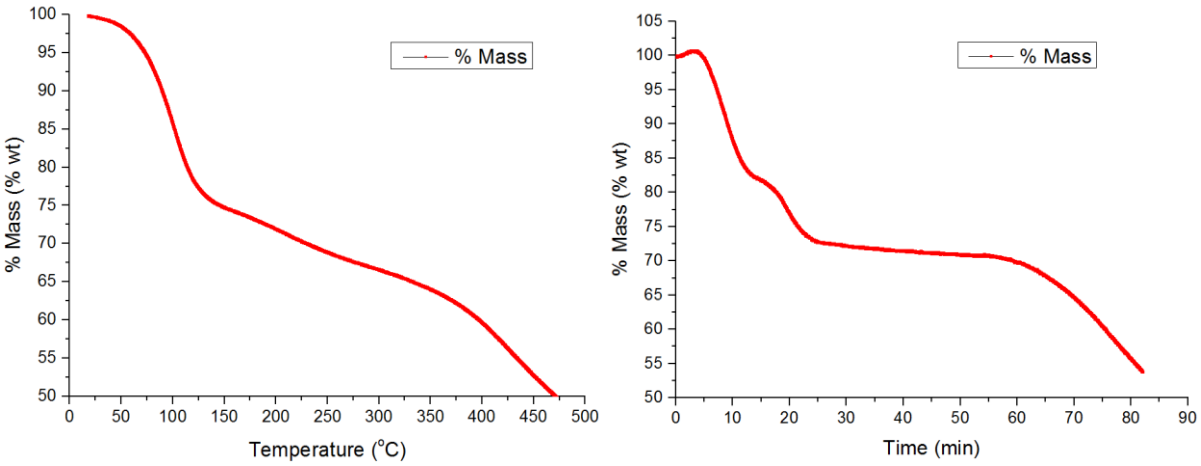

Figs 31 and 32. MIL-101 (Cr) TGA test from 20 to 600 °C and test from 20 to 450 °C, holding temperature at 250 °C for 30 minutes, 5 °C min^{-1} under nitrogen. Checked with literature [1].

UiO-66

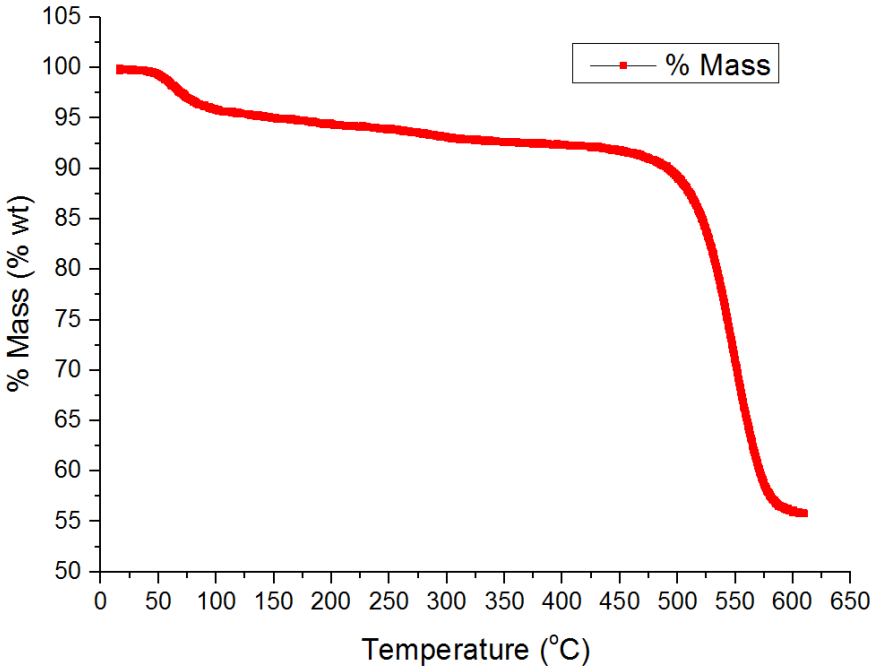

Fig 33. UiO-66 TGA test from 20 to 600 °C, 5 °C min^{-1} under nitrogen.

UiO-67

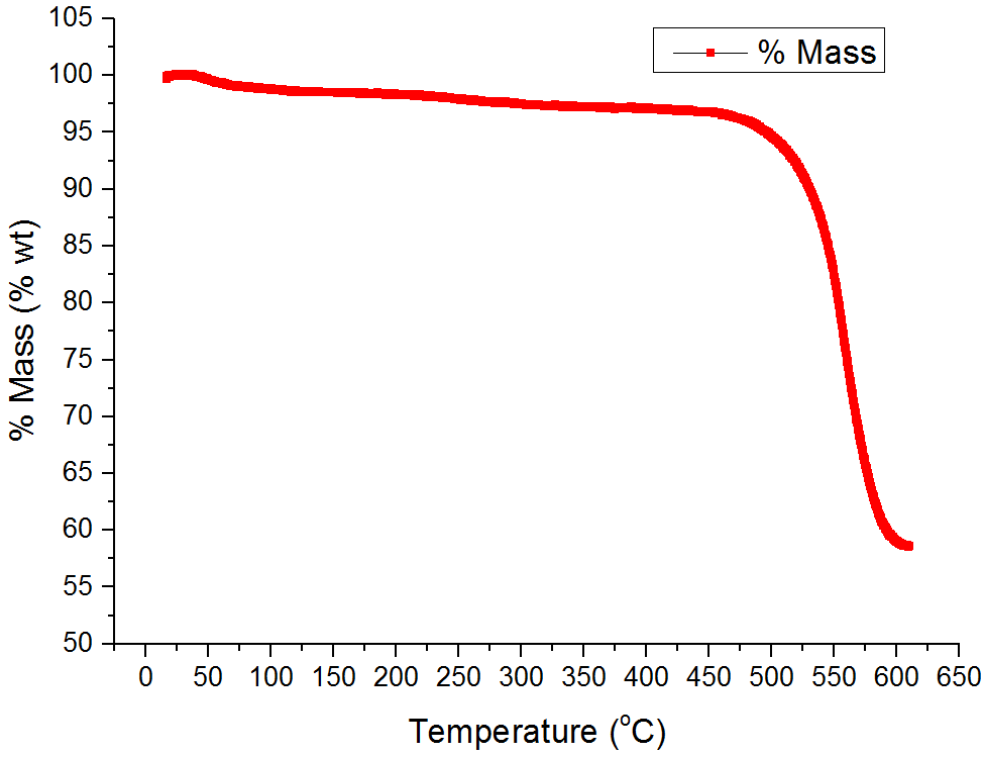

Fig 34. UiO-67 TGA test from 20 to 600 °C, 5 °C min^{-1} under nitrogen.

HKUST-1

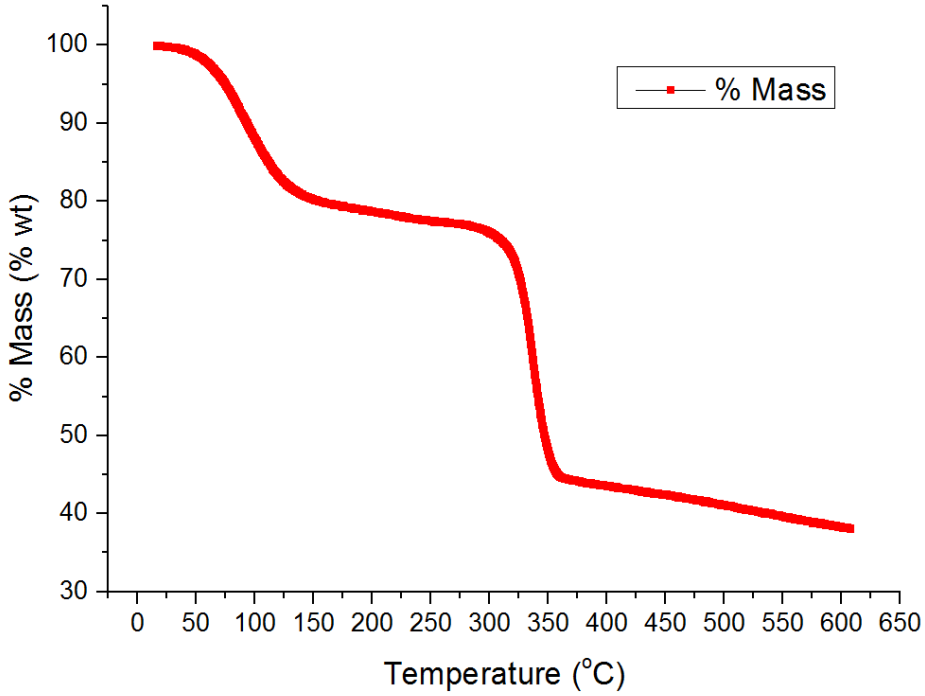

Fig 35. HKUST-1 TGA test from 20 to 600 °C, 5 °C min^{-1} under nitrogen. Compared with literature [39].

References

1. Ferey G., M.-D.C., Serre C., Millange F., Dutour J., Surble S., Margiolaki, I., *A chromium terephthalate-based solid with unusually large pore volumes and surface area.* Science, 2005. **309**(5743): p. 2040-2042.
2. Jiang, D.M., Keenan, L. L., Burrows, A. D., Edler, K. J., *Synthesis and post-synthetic modification of MIL-101(Cr)-NH2 via a tandem diazotisation process.* Chemical Communications, 2012. **48**(99): p. 12053-12055.
3. Yaghi, O., Eddaoudi, M., Li, H., Kim, J., Rosi, N., *Isoreticular metal-organic frameworks, process for forming the same, and systematic design of pore size and functionality therein, with application for gas storage*. 2003, Google Patents.
4. He M., Y.J.F., Liu Q., Zhong Z. X., Wang H. T., *Toluene-assisted synthesis of RHO-type zeolitic imidazolate frameworks: synthesis and formation mechanism of ZIF-11 and ZIF-12.* Dalton Transactions, 2013. **42**(47): p. 16608-16613.
5. Cravillon, J., Munzer, S., Lohmeier, S. J., Feldhoff, A., Huber, K., Wiebcke, M., *Rapid Room-Temperature Synthesis and Characterization of Nanocrystals of a Prototypical Zeolitic Imidazolate Framework.* Chemistry of Materials, 2009. **21**(8): p. 1410-1412.
6. Biswal, B.P., T. Panda, and R. Banerjee, *Solution mediated phase transformation (RHO to SOD) in porous Co-imidazolate based zeolitic frameworks with high water stability.* Chemical Communications, 2012. **48**(97): p. 11868-11870.
7. Cavka J.H., J.S., Olsbye U., Guillou N., Lamberti C., Bordiga S., Lillerud K.P., *A new zirconium inorganic building brick forming metal organic frameworks with exceptional stability.* Journal of the American Chemical Society, 2008. **130**(42): p. 13850-13851.
8. Serra-Crespo, P., Ramos-Fernandez, E. V., Gascon, J., Kapteijn, F., *Synthesis and Characterization of an Amino Functionalized MIL-101(Al): Separation and Catalytic Properties.* Chemistry of Materials, 2011. **23**(10): p. 2565-2572.
9. Eddaoudi, M., et al., *Systematic design of pore size and functionality in isoreticular MOFs and their application in methane storage.* Science, 2002. **295**(5554): p. 469-472.
10. He, M., et al., *Toluene-assisted synthesis of RHO-type zeolitic imidazolate frameworks: synthesis and formation mechanism of ZIF-11 and ZIF-12*. Dalton Transactions, 2013. **42**(47): p. 16608-16613.
11. Larabi, C. and E.A. Quadrelli, *Titration of Zr3(μ-OH) Hydroxy Groups at the Cornerstones of Bulk MOF UiO-67, [Zr6O4(OH)4(biphenyldicarboxylate)6], and Their Reaction with [AuMe(PMe3)]*. European Journal of Inorganic Chemistry, 2012. **2012**(18): p. 3014-3022.
12. Ferey, G., et al., *A chromium terephthalate-based solid with unusually large pore volumes and surface area.* Science, 2005. **309**(5743): p. 2040-2042.
13. Wong-Foy, A.G., A.J. Matzger, and O.M. Yaghi, *Exceptional H2 saturation uptake in microporous metal-organic frameworks.* Journal of the American Chemical Society, 2006. **128**(11): p. 3494-3495.
14. Millward, A.R. and O.M. Yaghi, *Metal-organic frameworks with exceptionally high capacity for storage of carbon dioxide at room temperature.* Journal of the American Chemical Society, 2005. **127**(51): p. 17998-17999.
15. First, E.L. and C.A. Floudas, *MOFomics: Computational pore characterization of metal-organic frameworks.* Microporous and Mesoporous Materials, 2013. **165**: p. 32-39.
16. Rowsell, J.L.C. and O.M. Yaghi, *Effects of functionalization, catenation, and variation of the metal oxide and organic linking units on the low-pressure hydrogen adsorption properties of metal-organic frameworks.* Journal of the American Chemical Society, 2006. **128**(4): p. 1304-1315.
17. Morris, W., Taylor, R. E., Dybowski, C., Yaghi, O. M., Garcia-Garibay, M. A., *Framework mobility in the metal-organic framework crystal IRMOF-3: Evidence for aromatic ring and amine rotation.* Journal of Molecular Structure, 2011. **1004**(1-3): p. 94-101.
18. Yoo, Y. and H.K. Jeong, *Generation of covalently functionalized hierarchical IRMOF-3 by post-synthetic modification.* Chemical Engineering Journal, 2012. **181**: p. 740-745.
19. Eddaoudi M., K.J., Rosi N., Vodak D., Wachter J., O'Keeffe M., Yaghi O.M., *Systematic design of pore size and functionality in isoreticular MOFs and their application in methane storage.* Science, 2002. **295**(5554): p. 469-472.
20. Tranchemontagne, D.J., Park, K.S., Furukawa, H., Eckert, J., Knobler, C.B., Yaghi, O.M., *Hydrogen Storage in New Metal-Organic Frameworks.* Journal of Physical Chemistry C, 2012. **116**(24): p. 13143-13151.
21. Peterson, G.W., et al., *Evaluation of MOF-74, MOF-177, and ZIF-8 for the removal of toxic industrial chemicals.* Chemical Biological Center. U.S. Army Research, Development and Engineering Command, 2008.

22. Furukawa, H., M.A. Miller, and O.M. Yaghi, *Independent verification of the saturation hydrogen uptake in MOF-177 and establishment of a benchmark for hydrogen adsorption in metal-organic frameworks.* Journal of Materials Chemistry, 2007. **17**(30): p. 3197-3204.
23. Saha, D. and S. Deng. *Hydrogen adsorption properties and structural stability of metal-organic framework (MOF)-177*. in *AIChE Annual Meeting, Conference Proceedings*. 2008.
24. Li, Y. and R.T. Yang, *Gas adsorption and storage in metal-organic framework MOF-177.* Langmuir, 2007. **23**(26): p. 12937-12944.
25. Jiang, D.M., A.D. Burrows, and K.J. Edler, *Size-controlled synthesis of MIL-101(Cr) nanoparticles with enhanced selectivity for CO2 over N-2.* Crystengcomm, 2011. **13**(23): p. 6916-6919.
26. Streppel, B. and M. Hirscher, *BET specific surface area and pore structure of MOFs determined by hydrogen adsorption at 20 K.* Physical Chemistry Chemical Physics, 2011. **13**(8): p. 3220-3222.
27. Lin, K.S., Adhikari, A. K., Su, Y. H., Shu, C. W., Chan, H. Y., *Synthesis, characterization, and hydrogen storage study by hydrogen spillover of MIL-101 metal organic frameworks.* Adsorption-Journal of the International Adsorption Society, 2012. **18**(5-6): p. 483-491.
28. Park K. S., N.Z., Cote A.P., Choi J.Y., Huang R.D., Uribe-Rom, F.J., Chae H.K., O'Keeffe M., Yaghi O.M., *Exceptional chemical and thermal stability of zeolitic imidazolate frameworks.* Proceedings of the National Academy of Sciences of the United States of America, 2006. **103**(27): p. 10186-10191.
29. Zhang, Z.J., Xian, S. K., Xia, Q. B., Wang, H. H., Li, Z., Li, J., *Enhancement of CO2 Adsorption and CO2/N2 Selectivity on ZIF-8 via Postsynthetic Modification.* Aiche Journal, 2013. **59**(6): p. 2195-2206.
30. Li, Q. and H. Kim, *Hydrogen production from NaBH4 hydrolysis via Co-ZIF-9 catalyst.* Fuel Processing Technology, 2012. **100**: p. 43-48.
31. Battisti, A., S. Taioli, and G. Garberoglio, *Zeolitic imidazolate frameworks for separation of binary mixtures of CO2, CH4, N2 and H2: A computer simulation investigation.* Microporous and Mesoporous Materials, 2011. **143**(1): p. 46-53.
32. Morris, W., He, N., Ray, K. G., Klonowski, P., Furukawa, H., Daniels, I. N., Houndonougbo, Y. A., Asta, M., Yaghi, O. M., Laird, B. B., *A Combined Experimental-Computational Study on the Effect of Topology on Carbon Dioxide Adsorption in Zeolitic Imidazolate Frameworks.* Journal of Physical Chemistry C, 2012. **116**(45): p. 24084-24090.
33. Chavan, S., Vitillo, J. G., Gianolio, D., Zavorotynska, O., Civalleri, B., Jakobsen, S., Nilsen, M. H., Valenzano, L., Lamberti, C., Lillerud, K. P., Bordiga, S., *H-2 storage in isostructural UiO-67 and UiO-66 MOFs.* Physical Chemistry Chemical Physics, 2012. **14**(5): p. 1614-1626.
34. Roy, A., Srivastava, AvanishK, S., Beer, S., Dilip, M., T.H., Gutch, P.K., Halve, A.K., *Degradation of sarin, DEClP and DECNP over Cu-BTC metal organic framework.* Journal of Porous Materials, 2013. **20**(5): p. 1103-1109.
35. Wang, Z.Q., K.K. Tanabe, and S.M. Cohen, *Tuning Hydrogen Sorption Properties of Metal-Organic Frameworks by Postsynthetic Covalent Modification.* Chemistry-a European Journal, 2010. **16**(1): p. 212-217.
36. Ardelean, O., Blanita, G., Borodi, G., Mihet, M., Coros, M., Lupu, D., *On the enhancement of hydrogen uptake by IRMOF-8 composites with Pt/carbon catalyst.* International Journal of Hydrogen Energy, 2012. **37**(9): p. 7378-7384.
37. Mu, L., et al., *A novel method to improve the gas storage capacity of ZIF-8.* Journal of Materials Chemistry, 2012. **22**(24): p. 12246-12252.
38. Bromberg, L., et al., *Chromium(III) Terephthalate Metal Organic Framework (MIL-101): HF-Free Synthesis, Structure, Polyoxometalate Composites, and Catalytic Properties.* Chemistry of Materials, 2012. **24**(9): p. 1664-1675.
39. Yan, X.L., et al., *Extremely enhanced CO2 uptake by HKUST-1 metal-organic framework via a simple chemical treatment.* Microporous and Mesoporous Materials, 2014. **183**: p. 69-73.
40. Servalli, M., M. Ranocchiari, and J.A. Van Bokhoven, *Fast and high yield post-synthetic modification of metal-organic frameworks by vapor diffusion.* Chemical Communications, 2012. **48**(13): p. 1904-1906.
41. Nguyen, L.T.L., Nguyen, C. V., Dang, G. H., Le, K. K. A., Phan, N. T. S., *Towards applications of metal-organic frameworks in catalysis: Friedel-Crafts acylation reaction over IRMOF-8 as an efficient heterogeneous catalyst.* Journal of Molecular Catalysis a-Chemical, 2011. **349**(1-2): p. 28-35.